Pharmacokinetic Perfusion Curves Estimation for Liver Tumor Diagnosis from DCE-MRI

Liliana L. Caldeira and João M. Sanches*

Instituto de Sistemas e Robótica / Instituto Superior Técnico
1049-001 Lisbon, Portugal

Abstract. *Dynamic-Contrast Enhanced MRI* (DCE-MRI) is a method to analyze the perfusion dynamics in the tissues. The contrast agent concentration along the time, after the bolus injection, depends on the type of tissue observed, namely on its vascularization density and metabolic activity. The number of acquired volumes in this type of exam is usually very small, typically < 10, and the volumes are misaligned due to respiratory and cardiac activities.

In this paper an algorithm to automatically characterize the malignancy of the tumor is presented based on the perfusion curves on each voxel of the tumor, obtained from DCE-MRI. A non-rigid registration procedure based on *Mutual Information* (MI) criterion is used to align the the small volumes representing the *region of interest* (ROI) containing the tumor along the time. A *pharmacokinetic* (PK) third order linear model is estimated from the observations and its parameters are used to classify the malignancy of tumor.

1 Introduction

DCE-MRI is used to get information about the malignant tissues that generally have an earlier contrast uptake, with rapid and large increases compared with benign tissues. The slopes before and after the maximum of the curve, called *WashIn* and *WashOut*, respectively, are used to classify the tumor with respect to its malignancy. Cancer tissues present rapid and higher amplitude *WashIn* and *WashOut* rates than healthy tissues allowing the evaluation of the tumor perfusion and DCE-MRI is the preferred technique to measure them. However MRI image processing and reconstruction is usually computationally intensive and time consuming. Faster processing can be achieved by restricting the volume to a smaller ROI containing the tumor.

In this paper, an algorithm is presented to cope with this data. Processing these such small regions leads to difficulties concerning the registration procedure. The motion occurred during the acquisition due to respiratory and cardiac activity must be considered to make it possible to follow the same voxel along

* This work was supported by Fundação para a Ciência e a Tecnologia (ISR/IST pluriannual funding) through the POS Conhecimento Program which includes FEDER funds.

A. Campilho and M. Kamel (Eds.): ICIAR 2008, LNCS 5112, pp. 789–797, 2008.

the whole time course. The perfusion curves are estimated from MRI signal intensity contrast enhanced. Pharmacokinetics (PK) models are used to quantify perfusion in a physiological meaningful way. In this paper, parameters of a PK model are estimated from the observed intensity profiles as well as the initial position and duration of the bolus injection (which are not usually accurately known) to compute the *WashIn* and *WashOut* parameters.

PK models assume that the contrast agent is distributed between two main tissue compartments: the *intra-vascular plasma volume space* and the *extravascular extracelular space* (EES). The generalized kinetic model, describing the evolution of contrast agent concentration with time, is defined by the following differential equation [1],

$$dC_{tumor}/dt = K_{trans}C_p - K_{ep}C_{tumor} \tag{1}$$

where C_{tumor} and C_p are the concentration of the contrast agent in EES and plasma space, respectively. K_{trans} and K_{ep} are constants that may be use to classify tumors. However, usually the *Wash* rates among others are the preferred parameters in clinical practice for sake of simplicity [2]. The PK model is estimated from the *arterial input function* (AIF), measured in one of the arteries around the tumor, and the observed contrast agent concentrations. However, since small regions are being used no arteries are available to measure the AIF, which mean it must be also estimated. Therefore, in this paper the whole chain, AIF and PK systems are modeled [1] as an only poles three order *linear time invariant* (LTI) system.

2 Problem Formulation

In this paper, the volumes are assumed to be continuous functions evolving in the continuous time, $f(x,t) : \Omega \rightarrow R$ where $\Omega \subset R^3 \times R$. The function $f(x,t)$ is described by a linear combination of basis functions as follows: $f(x,t) = \sum_p f_p \phi_p(x,t)$ where $p \in N^4$ and f_p are coefficients to be estimated. The observation intensities and respective locations and times are arranged in the matrices $Z = \{z_i\}$, $X = \{x_i\}$ and $T = \{t_i\}$ respectively where $0 \leq i \leq L$ and L is the number of observations.

The proposed algorithm is composed by six main steps: i) MRI acquisition, ii) ROI selection (crop), iii) non rigid transformation register of the volumes, iv) PK model parameter estimation, v) perfusion curves estimation from each *time course* associated with each voxel and vi) tumor malignancy classification.

2.1 Registration

The Registration procedure performed in the volumes is needed to compensate organ and tissue displacements occurred during acquisition. Here, the MI [1] criterion is maximized by geometrically transforming each volume in a pairwise basis:

$$\widehat{T} = \arg\max_T MI\left[f(x,p), f(T(x,q))\right] \tag{2}$$

where $f(x,p)$ and $f(x,q)$ are two volumes from the data sequence. This process is time consuming and computationally intensive where MI is defined as follows:

$$MI(f,g) = h(f) + h(g) - h(f,g) \tag{3}$$

where $h(z) = -E_z(\ln p(z))$ is the entropy of z and $E_z()$ is the expectation operator.

In order to reduce the processing time, a small ROI is selected from the whole volume. This procedure increases the difficulty of the registration process because there are less samples available. The marginal and joint probability densities functions are estimated by using the Parzen method.

2.2 PK Model

PK models are useful to describe contrast agent concentration, which is in general not easy directly measured. Therefore, an intensity based classification algorithm is preferred since contrast agent concentration values are difficult to assess precisely. In the case of a low-molecular weight contrast agent, the relation between intensity and contrast agent concentration is the following $s(t) = s(0)\cdot(1+g\cdot C(t))$ where $s(t)$ is the signal intensity, $C(t)$ is the correspondent concentration value, $s(0)$ is the baseline intensity and g is a parameter depending on the tissue and contrast agent. Since there are no measures for the g parameter, the signal

$$y(t) = g \cdot C(t) = s(t)/s(0) - 1 \tag{4}$$

is used instead of the concentration itself $C(t)$ [3]. In this paper, a time invariant linear discrete PK model is used in which the contrast agent concentration is modeled as a response to the AIF, proposed in [4]. Unfortunately in a small ROI, the AIF is not available because there are no arteries in the cropped volume. To overcome this difficulty, the AIF is also estimated and modeled as the response of a second order system to the bolus injection (in the arm) since it is assumed to be a bi-exponential. The PK model input is the bolus injection, $u(t)$ and the output is the contrast signal, $y(t)$. This two serial block model is represented in Fig. 1 where the first one represents the diffusion of contrast agent into the artery near the tumor and the second block represents the contrast agent exchanges between the artery and the tumor. This last block is based on the multi-compartment model - the vascular space and the EES [5] described by Eq. (1). The goal is to estimate the parameters describing the model from the low temporal resolution intensity profiles for each voxel in the ROI.

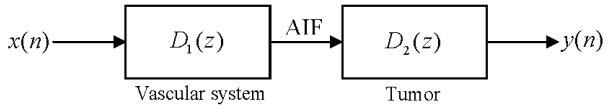

Fig. 1. PK model

3 Estimation

In this section, the PK model parameters estimation procedures are described. The MI is estimated from the observations. Here the *Mattes MI* (from *ITK* framework) is used where all observations are not used in order to speed up the process. Therefore, the selection of the representative samples and the number of discrete bins used to represent the histograms are key issues when tunning the algorithm [6]. This topic is described later.

The equivalent discrete overall system obtained form in Eq.(4) and form the AIF, represented in Fig. 1, is the following

$$H(z) = \frac{Y(z)}{X(z)} = \frac{K}{(1 - az^{-1})(1 - bz^{-1})(1 - cz^{-1})} \tag{5}$$

The correspondent differences equation is

$$y(n) = Kx(n) - Ay(n-1) - By(n-2) - Cy(n-3) \tag{6}$$

where $A = 1 - a - b - c$, $B = ab + ac + bc$ and $C = -abc$.

In this section, a single time course is considered where $\mathbf{z} = \{z(0), z(1), ..., z(N-1)\}^T$ is the vector containing the expanded observations of a single voxel along the time, after alignment. This expanded data is obtained by inserting new observations in new instants by interpolating the real observations.

$\mathbf{u} = \{u(0), u(1), ..., u(N-1)\}^T$ is the bolus injection signal and $\theta = \{K, A, B, C\}^T$ is the vector of parameter to be estimated. The estimation of θ is performed with the *Shank's* method [7] given $\mathbf{z}$ and $\mathbf{u}$. This method provides the θ vector defining the third order system that best represents the relation between u and z in the MSE sense.

The bolus injection $u(n)$ is not known and must be estimated. Three constrains are assumed, i) $u(n) = 1$ for $d_0 \leq n \leq d_1$ with d_0 and d_1 unknown, ii) the bolus injection starts before the acquisition of the first volume enhanced and iii) the duration of the injection has to be < 40 seconds. The estimation of parameters d_0 and d_1 is performed by testing all admissible values and choosing the ones that lead to a minimum error $[\hat{d}_0, \hat{d}_1] = \arg\min_{d_0,d_1} \|z - h * u(d_0, d_1)\|$ where it is assumed that $z(n) = 0$ for $0 \leq n < d_0$. It is also forced that the $y(n)$ will approximate zero around 960 seconds after the beginning of the acquisition when the contrast agent *Gadolinium* (Gd) is taught to be going out of the body.

After the estimation of $\mathbf{u}$ (duration and start point) the perfusion curves and *WashIn* and *WashOut* rates are analytically estimated estimated from the estimated PK model.

4 Experimental Results

In this section, we present results with real DCE-MRI data. This algorithm was implemented using C++ supported with the open source *Insight Segmentation and Registration Toolkit* (ITK) and *Visualization toolkit* classes (VTK) and Matlab.

DCE-MRI acquisition is started with the intravenous administration of about 20-25 ml of Gd contrast medium in the arm using an automatic injector. To minimize organ motion, breath-hold is asked to the patients during acquisitions. The patients underwent DCE-MRI imaged with a Siemens Sonata scanner using the "Vibe FS tra BH post iPat" protocol. Two dataset are used which are composed by a sequence of six volumes, approximately 512x800x64 voxels each. The interval between the single pre-contrast volume and the first pos-contrast one is 120 seconds and the interval between the next ones is 30 seconds. The voxel size varies from $0.72 \times 0.72\ mm^2$ to $0.78 \times 0.78\ mm^2$ and the slices are from 2-3 mm thick. The acquired images are retrieved from the MR scanner via DICOM protocol. The first dataset corresponds to a malign tumor and the second one is benign. This classification was provided by several medical doctors, specialists in the area.

The same rectangular ROI, around the tumor, is used in all sequences. The cropped size is about $50 \times 40 \times 10$ for small tumors (Data Set 1) and $80 \times 90 \times 16$ for larger ones (Data Set 2). One of the consequences of a ROI selection is dynamic range reduction of the images. The dynamic range in the cropped volume is smaller than in the whole volume making it possible to use smaller number of bins in the registration step, leading to a decreasing in the processing time.

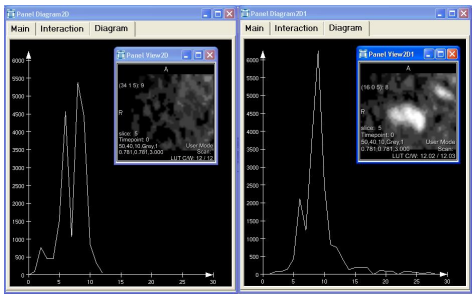

Fig. 2. Fixed and Moving Image and its Histograms

4.1 Optimal Number of Bins and Samples in the Registration

The number of bins and samples is critical in the representation of the true probability density functions. It was concluded that a number of bins greater than half of the largest dynamic range leads to approximately the same results. In order to reduce even more the processing time only a partial amount of voxels are used in the histogram estimation. A simple heuristic is proposed based in the following: if the event F is the updating action of a given bin then it is a Bernoulli trial. With this assumptions F follows a p mean normal distribution with standard deviation $p(1-p)/n$ where n is the number of the observations. For a confidence level of 95%, the error is $e = 1.96 \times \sqrt{p(1-p)/n}$. So the sample dimension that leads to an error less than e is $n = (1.96/e)^2 p(1-p)$.

Here $p = 1/L^2$ is used where L is the number of bins and the number of samples is chosen in order to make $e = 0.75\%$.

To access the previous heuristic, a set of experimental tests were performed for different values of n. Let $\alpha = N/n$ be a fraction of the total number of samples N. For each α the $MSE(\alpha) = \|MI(1) - MI(\alpha)\|$ was computed. The results of this experiment have shown that for $\alpha \geq 5\%$ the MSE value stabilizes. Therefore, here only 5% of the data is used in order to speed up the algorithm. This is represented in Figure 3.

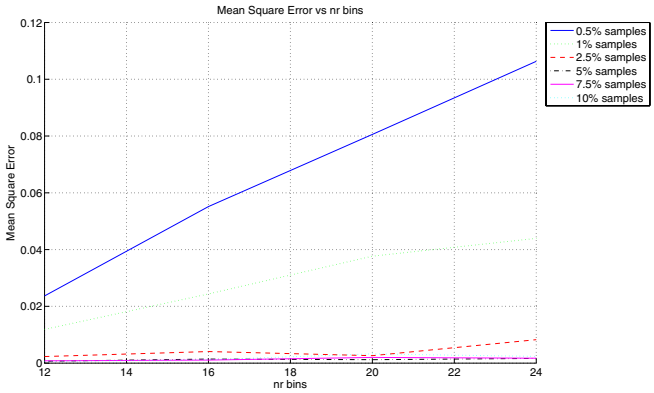

Fig. 3. Mean Square Error of estimates

4.2 Pairwise Registration Strategies

The MI registration procedure is pairwise based which means a series of two volumes alignments are performed in order to achieve a global alignment. The strategy to chose each pair for alignment is relevant for the final results. Here, three strategies were tested: i) sequential, ii) reference and iii) random. In the first case, every two consecutive volumes are aligned in a sequential order. In the reference strategy, all volumes but one are aligned with the reference volume. In the last strategy, the pairing is performed in a random basis. Here, the stop criterion is the MI obtained with the best of the two other approaches. These three approaches were compared based on processing time and MI values (see Table 1).

Table 1. Alignement results

Image Set 1 $50 \times 40 \times 10$ size 12 bins, 1000 samples		
	Time (sec)	MI
Sequential	236	-0.1198
Reference	236	-0.5458
Random	204	-0.55

It is concluded that the random way for small dimension volumes is faster than the other two methods. This is no longer true for larger volumes due to the resampling procedure which is time consuming and is typically performed more times in the random approach. Each Image Set was registered with the best approach for the following algorithms.

4.3 PK Models

The small number of experimental points was increased by a shape-preserving piecewise cubic interpolation. These curves and experimental data, extracted from healthy and non-healthy tissues. The perfusion curves of the two datasets were obtained in 36 voxels around the center of the image/tumor. This results can be seen in Figure 4. These curves are how it was expected and we can already see that different tumors have different perfusion curves when comparing the different datasets.

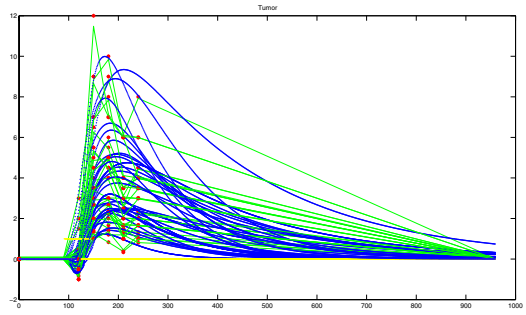

(a) Malign (Data Set 1)

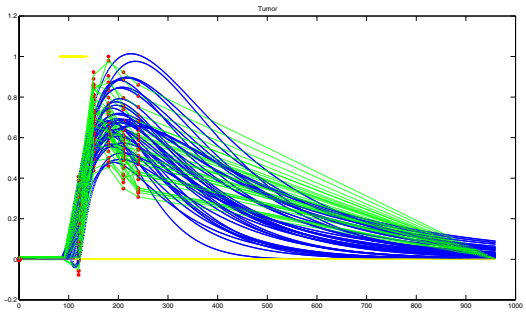

(b) Benign (Data Set 2)

Fig. 4. Perfusion Curves. Observations (red), experimental points(green) , bolus Injection (yellow) and Modeled Perfusion(blue))

Table 2. DataSet Results

Data Set 1: $50 \times 40 \times 10$ size 12 bins, 1000 samples		
	Mean	Var
WashIn	0.1394	0.0054
WashOut	-0.0178	$1.26E-04$
Data Set 2: $80 \times 90 \times 16$ size 32 bins, 7000 samples		
	Mean	Var
WashIn	0.0166	$1.57E-05$
WashOut	-0.0024	$3.60E-07$

The two features: WashIn and WashOut of the perfusion curves for each pixel were computed. It is known that malign tumors are more heterogeneous than benign ones.

The mean and variance for each dataset are also computed to study the heterogeneity of the tumor. Data set 2 presents smaller variances in the two features as well the mean values. This shows that this data set has a lower heterogeneity in the tumor tissue.

5 Conclusions

In this work, a MI based registration algorithm was developed using non-rigid transformations for DCE-MRI datasets. With a small ROI, small temporal resolution, optimal number of bins and samples leads to an optimized algorithm from a time and computational point of view. Several global registration strategies based in several pairwise alignment methods were also tested. PK models estimated from the resulting 1D time courses, associated to each voxel, were used to automatically get information to classify tumors based on the *WashIn* and *WashOut* rates obtained from the perfusion curves. In the future, these *WashIn* and *WashOut* rates should be calculated from different tissues and individuals (a training dataset with more variance) in order to design more robust classifiers.

References

1. Tofts, P.S.e.a.: Estimating kinetic parameters from dynamic contrast-enhanced T(1)-weighted MRI of a diffusable tracer: standardized quantities and symbols. J. Magn. Reson. Imaging 10(3), 223–232 (1999)
2. Gal, Y., Mehnert, A., Bradley, A., McMahon, K., Crozier, S.: An evaluation of four parametric models of contrast enhancement for dynamic contrast magnetic resonance imaging of the breast. In: Proceedings of the 29th Annual International Conference of the IEEE EMBS (2007)
3. Port, R.E., Knopp, M.V., Brix, G.: Dynamic contrast-enhanced MRI using Gd-DTPA: interindividual variability of the arterial input function and consequences for the assessment of kinetics in tumors. Magn. Reson. Med. 45(6), 1030–1038 (2001)

4. Collins, D.J., Padhani, A.R.: Dynamic magnetic resonance imaging of tumor perfusion. Approaches and biomedical challenges. IEEE Eng. Med. Biol. Mag. 23(5), 65–83 (2004)
5. Srikanchana1, R., Thomasson, D., Choyke, P., Dwyer, A.: A comparison of pharmacokinetic models of dynamic contrast enhanced mri. In: Proceedings of the 17th IEEE Symposium on Computer-Based Medical Systems (CBMS 2004) (2004)
6. Pluim, J., Maintz, J., Viergever, M.: Mutual-information-based registration of medical images: a survey. IEEE Transactions on Medical Imaging 22(8), 986–1004 (2003)
7. Shanks, J.L.: Recursion filters for digital processing. Geophysics 32, 33–51 (1967)